Applications of System Identification Methods to the Prediction of Helicopter Stability, Control and Handling Characteristics

G. D. Padfield
RAE Bedford, UK

R. W. DuVal
NASA - Ames Research Center

Abstract

The paper describes a set of results from the first phase of an RAE/NASA collaborative programme on rotorcraft system identification that has the main objective of improving prediction methods. Flight measurements collected at RAE Bedford on an experimental Puma helicopter are reviewed and some notable characteristics highlighted. Following a brief review of previous work in rotorcraft system identification, the results of state estimation and model structure estimation processes applied to the Puma data are presented. The results, which were obtained using NASA developed software, are compared with theoretical predictions of roll, yaw and pitching moment derivatives for a 6 degree of freedom model structure. Anomalies reported in other investigations have reappeared in this study. The theoretical methods used are described in the Appendix where a framework for reduced order modelling is outlined.

Notation

A	-state matrix (equation (7))
B	-control matrix (equation (7))
C_{Qi}	-rotor induced torque coefficient (equation (10))
C_T	-rotor thrust coefficient (equation (3))
C_{YFN}	-fin sideforce coefficient (Fig 5)
$\underset{\sim}{F}$	-force and moment vector (equation (7))
g	-gravitational acceleration
h_R	-height of aircraft cg below rotor (ft,m) (equation (7))
I_{xx}, I_{yy}, I_{zz}	-moments of inertia of aircraft in roll, pitch and yaw (slugs ft^2, kg m^2)
L_v, L_p etc	-rolling moment concise derivatives (normalised by I_{xx})
M_u, M_w etc	-pitching moment derivatives (normalised by I_{yy})
$M_{\beta_{1c}}$	-pitching moment derivative wrt flapping (normalised by I_{yy})
N_v, N_r etc	-yawing moment derivatives (normalised by I_{zz})
N_{Ri}	-yawing moment from main rotor (normalised by I_{zz})
p, q, r	-roll, pitch and yaw rates (rad/s)
R	-rotor radius (ft,m)
R^2	-(multiple correlation coefficient)^2
s	-solidity
$T_{\frac{1}{2}}$	-time to half amplitude (s)
U_e, W_e	-trim values of aircraft forward and normal velocity components (ft/s, m/s)
u, v, w	-velocity perturbations along body x,y and z axes (ft/s, m/s)
v_o, w_o	-sideways and vertical velocity components (ft/s, m/s)
$\underset{\sim}{u}$	-control vector (equation (7))
$\underset{\sim}{x}$	-state vector (equation (7))
β	-sideslip angle (rad)
β_{1c}, β_{1s}	-rotor longitudinal and lateral disc tilts respectively (equation (1))
γ	-Lock number (equation (1))
ζ	-relative damping
η_{1s}, η_{1c}	-longitudinal and lateral stick position (% aft, std)
η_p	-pedal position (% left)
θ_{1s}, θ_{1c}	-longitudinal and lateral cyclic pitch angles (equation (1))
θ	-aircraft pitch angle
λ	-system eigenvalue
λ_o	-rotor downwash (normalised) velocity (equation (10))
λ_β	-flap frequency ratio
μ_z	-normal velocity component at rotor disc (equation (10))
ρ	-air density
σ	-relative air density
ϕ	-aircraft roll angle
Ω	-rotorspeed
ω_o	-dutch rollfrequency (equation (9))

Introduction

A collaborative programme between the Royal Aircraft Establishment and the NASA - Ames Research Center to develop and exchange information on rotorcraft system identification is now underway with the main objective of improving prediction methods. In the first exercise of this kind at RAE, flight tests have been made on a Puma helicopter and the results have been analysed at NASA - Ames, using software developed in support of the Rotor Systems Research Aircraft programme. This paper reports on the first phase of this activity. The paper begins by describing the aircraft and data processing system at RAE Bedford and attempts a preliminary interpretation of selected flight data based on comparison with theory. Aspects of rotorcraft system identification are then reviewed and the techniques currently in use are described.

Derivatives, estimated by these techniques for the Puma at a nominal 100 kn trim condition, are presented and compared with results predicted by a linear, 6 degree of freedom theoretical model developed at RAE[1]. Some of the major anomalies are discussed. Finally the use of reduced order linear models for handling studies is reviewed, and approximations to the natural modes discussed in some detail.

Flight Mechanics Investigations with Puma XW 241 at RAE Bedford

The Aircraft and Data Processing System

Puma XW 241 (Fig 1) is a multi-purpose experimental aircraft operated and managed by the Helicopter Section of the Flight Research Division at RAE Bedford. Since its procurement in 1974, the Puma has been used in a variety of research programmes and has recently been fitted with a digital Pulse Code Modulated (PCM) recording system; the results described in this paper were obtained with this equipment. A block diagram highlighting the features of the current data acquisition and processing system is shown in Fig 2.

The instrumentation system includes three packs of linear accelerometers of both ac pickoff and force feedback type, two packs of rate and attitude gyros and a heading gyro. Air data sensors give airspeed measurement from a conventional pitot static and incidence and sideslip angles from vanes located on a nose boom. All four control displacements, the three swash plate jacks and the tail rotor pitch jack are sensed by potentiometers. In addition, one of the four blades is currently instrumented to measure flap, lag and feather angles at the bearings. Sampling rates vary from 32 to 256 per second, the lower rate restricted to slowly varying quantities, *eg* airspeed. The current overall rate for the multiplexed system is 8024 words (12 bit) per second but the pattern of signals in each data field is flexible.

During the Spring of 1981 a trial was conducted with the object of data gathering for a system identification exercise. Trims and responses to pilot shaped control inputs over a range of flight conditions were recorded. Data tapes from one of these flights, designated 325, were sent to the Ames Research Centre for analysis using NASA software during the first round of the RAE/NASA collaborative programme in Rotorcraft Flight Mechanics. Results described in this paper are drawn from this exercise and used in subsequent interpretation, analysis and comparison with theory.

Data pertaining to the trim conditions for flight 325 are given in Table 1. The nominal trim IAS was 100 kn from which a series of shaped control inputs were made and the ensuing response measured and recorded. The inputs included steps, doublets and "3211" multisteps and generally produced repeatable response patterns; atmospheric conditions at the test points were very smooth.

Time to recovery varied with input type and size but typically step inputs gave about 10 s of data and 'return-to-trim' multisteps gave about 20-30 s duration.

Typical results from cyclic and pedal inputs are reproduced in Figs 3 and 4. Before introducing the system identification process a preliminary interpretation will be attempted on these results together with a limited comparison with theoretical predictions.

Preliminary Interpretation of Flight Results and Comparison with Theory

An initial assessment of the flight results and comparison with theory provides a suitable background to judge the effectiveness of both the theory itself and the system identification method, described later. The theoretical results presented in this paper are based on a 6 degree of freedom linearisation of the nonlinear simulation model described in Ref 1. During the development of this nonlinear model, a degree of validation was achieved through flight/theory comparisons of Puma data; these results are reported in Refs 1 and 2.

The short term pitch and roll rate response to longitudinal and lateral cyclic steps inputs respectively are shown in Fig 3. The comparisons with theory are encouraging and indicate that the principal damping, control sensitivity and 'static stability' parameters ought to be predicted with reasonable accuracy by theory. There is some evidence that the 'initial' angular acceleration is sharper in theory but this is to be expected with a quasi-steady rotor model. This phenomenon and the difficulties it can present to a derivative estimation process are discussed in more detail in the next section.

Turning now to the flight results shown in Fig 4, we see the coupled response to a doublet input applied to the pedal. This set of data reveals the presence of a lightly damped lateral/directional oscillation that was very apparent to the pilot and observer performing these tests. This oscillatory 'dutch roll' mode is also predicted by theory and a comparison of the measured and predicted characteristics is

shown in Table 2. It can be seen that the lateral/directional characteristics are roughly in agreement whereas the longitudinal couplings, particularly the phase relationships, are significantly different. Having established possible basic ingredients of this mode it is useful to examine the theory to determine the origins. The derivative matrix used in the analysis is given in Table 3 and the system eigenvalues in Table 4. Included in Table 4 are the longitudinal and lateral subsystem eigenvalues derived with coupling terms set to zero. Conventional fixed-wing aircraft terminology is used to describe the different modes. The frequency of the dutch roll oscillation is determined primarily by the directional stability, *ie*

$$\omega_{\text{dutch roll}} \sim \sqrt{U_e N_v} = 1.011 \text{ rad/s.}$$

An important effect displayed in Table 4 is the considerable reduction in damping of this mode when the coupling terms are included. The damping is rather low even for the lateral subsystem and this can largely be attributed to the low value of the yawing moment derivative N_v. This derivative contributes to the mode damping when the effective centre of the oscillation is a condition of non-zero sideslip. Wind tunnel data[3] for the Puma fin in sideslip, as used in the theoretical model, is shown in Fig 5. The sideforce is strongly nonlinear with sideslip, but over the range $-5^o < \beta < +8^o$, practically no lift is produced by the fin. It is believed that this effect is due to the suction on the rear of the 'lower surface' at small angles of attack; a characteristic of thick aerofoil sections with large trailing edge angles[4]. This aspect is discussed further in Ref 5, in relation to the Puma and how design improvements obviate the effect on the AS 332 Super Puma.

Returning to the coupled system, a sensitivity analysis reveals that the main coupling derivatives affecting the dutch roll damping are M_p and N_w. For a perfectly governed rotorspeed the derivative N_w reflects the torque changes produced by the powerplant, following rotorspeed variations due to incidence perturbations. The effect of this derivative on the dutch roll and longitudinal short period eigenvalues is illustrated in Fig 6. N_w is destabilising for the dutch roll mode and the roots are close to the longitudinal and lateral subset approximations when N_w is zero. Fig 7 illustrates how the phase relationship between w and r (incidence and yaw rate) perturbations vary with N_w for the dutch roll mode. They are seen to converge as N_w increases and clearly when they are in phase, torque reductions impose a positive yawing moment on the fuselage when the yaw rate is a maximum, giving a negative damping contribution. This effect is discussed in more quantitative terms in the Appendix. The above description of the increased instability of the lateral oscillation is dependent on the correct phase relationship between longitudinal and lateral variables. As highlighted earlier this is the area of most serious discrepancy between flight and theory. It should perhaps be emphasised that engine/rotor dynamics are not included in the theoretical model but that there is evidence[6] that including this degree of freedom can reduce the effective yaw damping. Included in Fig 4 is the main rotor torque variation (via shaft strain gauge measurement) during the oscillation. Although fairly noisy, the fluctuations are seen to be phased relative to yaw rate, so that as the aircraft is yawing to starboard, the engine is applying a clockwise torque (minimum) to the fuselage. This is in the same sense as predicted by theory and it may be surmised that the phase shift relative to pitch rate and vane oscillations is accounted for in the engine dynamics.

As a final note in this exploratory section some measurements were made on the Puma following a pedal doublet input with the pitch axis stability augmentation switched on, to give some indication of the effect of reducing the longitudinal coupling. A comparison of yaw and pitch vane responses with and without augmentation is shown in Fig 8. Clearly the damping of the oscillation has increased with the reduced longitudinal coupling. In fact, the time to half amplitude has now reduced to about one cycle, *ie* approximately the same as predicted by the lateral subset calculation. The frequency is practically unchanged. Longitudinal coupling obviously does play an important role in the damping of this oscillation.

Rotorcraft System Identification

The state of the art in the field of system identification has largely been developed in the fixed wing community, the most recent comprehensive review of which can be found in Ref 7. There have been several attempts to apply the various techniques to helicopters, a review of which also appears in Ref 7. Before describing the methods used in the RAE/NASA collaboration it is perhaps worth making a few observations on these past efforts and highlighting some of the lessons learned.

Observations on Previous Work

The ground rules for helicopter system identification were laid down in the pioneering work by Molusis in the early

seventies[8-10]. In his papers, Molusis emphasised the need for long data records and combined manoeuvres in order to provide sufficient information for reliable estimation. He also stressed the importance of providing satisfactory initial estimates of derivatives in maximum likelihood algorithms by using an optimal filter/smoother in conjunction with a least squares estimator. Of particular relevance to the helicopter problem were Molusis's observations on the effects of rotor/fuselage coupling on derivative estimation. These were clearly demonstrated by attempting an identification of a 6 degree of freedom (dof) model from simulation data that included rotor flapping modes[10]. The identified derivatives were substantially different from quasi-steady predictions even though time histories showed reasonable correlation. Including the three principal multi-blade coordinates in the assumed model and performing the reduction to a 6 dof model after the identification, resulted in very good agreement with quasi-steady values. The conclusion was not that 6 dof quasi-steady theoretical models were necessarily inadequate but that profound difficulties could be expected in trying to estimate these from flight measurements of fuselage motion alone. Molusis suggested an empirical correction based on computed theoretical data but his own results showed that this was not very satisfactory[10]. A perusal of the simulation results in Ref 10 reveals that perhaps the most serious discrepancy is the underestimation of the primary rate damping derivatives by the 6 dof identification. These usually produce dominant effects about all axes and relatively simple theory should be fairly reliable. A gross underestimation of this effect will obviously lead to a further corruption of secondary effects in each equation when the time histories are forced to agree. A possible cause of this anomaly can be demonstrated by a fairly simple example.

Consider a hovering rotor with zero flapping hinge offset and centre of gravity (cg) on the rotor shaft. The first order flapping equations in multi blade coordinates β_{1c} and β_{1s}, that represent longitudinal and lateral disc tilt respectively, can be written as

$$\begin{bmatrix} 1 & \frac{16}{\gamma} \\ -\frac{16}{\gamma} & 1 \end{bmatrix} \begin{bmatrix} \beta_{1c} \\ \beta_{1s} \end{bmatrix} - \begin{bmatrix} 0 & -\Omega \\ \Omega & 0 \end{bmatrix} \begin{bmatrix} \beta_{1c} \\ \beta_{1s} \end{bmatrix} = \begin{bmatrix} \frac{16}{\gamma} p + \Omega\theta_{1c} + q \\ -\frac{16}{\gamma} q + \Omega\theta_{1s} + p \end{bmatrix} \quad \ldots\ldots(1)$$

where γ is the rotor Lock number, Ω the rotor speed, p and q the body roll and pitch rates and θ_{1s}, θ_{1c} the longitudinal and lateral cyclic pitch respectively. Non-uniform inflow effects have been neglected for this example. Constraining the body to rotate only in pitch and neglecting forward speed effects, the above equations can be augmented by the body pitching moment equation

$$\dot{q} = \frac{1}{I_{yy}} M_{\beta_{1c}} \beta_{1c} \qquad (2)$$

I_{yy} is the pitching moment of inertia and the pitching moment derivative $M_{\beta_{1c}}$ can be written in terms of the rotor thrust coefficient C_T,

$$M_{\beta_{1c}} = - h_R \rho (\Omega R)^2 \pi R^2 C_T \quad . \qquad (3)$$

Here h_R is the cg distance below the rotor, ρ the air density and R the rotor radius. For present purposes we have assumed in equation (3) that the rotor thrust remains normal to the disc during pitching motions. The quasi-steady form of equation (2) can be written in the form

$$\dot{q} = M_q q + M_{\theta_{1s}} \theta_{1s} \qquad (4)$$

where $M_q = \frac{M_{\beta_{1c}}}{I_{yy}} \frac{\partial \beta_{1c}}{\partial q}$, $M_{\theta_{1s}} = \frac{M_{\beta_{1c}}}{I_{yy}} \frac{\partial \beta_{1c}}{\partial \theta_{1s}}$ . .....(5)

From equation (1) the quasi-steady flapping derivatives can be written as

$$\frac{\partial \beta_{1c}}{\partial q} = 16/\gamma\Omega \quad , \qquad \frac{\partial \beta_{1c}}{\partial \theta_{1s}} = -1. \qquad (6)$$

To demonstrate the phenomenon in question we now attempt to estimate the derivatives M_q and $M_{\theta_{1s}}$ in a model structure given by equation (4) from data generated by equations (1) and (2), following a step input in θ_{1s}. Configuration data used for the numerical study are $\gamma = 8.0$, $\Omega = 27.8$ rad/s and $M_{\beta_{1c}}/I_{yy} = -6.36$. Using a least squares estimator, the effect of data length on the estimated derivatives is shown in Fig 9. A sampling interval of 0.04 s was used for this case. The effect is dramatic, particularly on the estimated damping M_q. Using only a short data length a positive M_q is predicted and even after 2 s the estimation is still only 70% of the quasi-steady value. For a 2 s data run, the effect of sampling interval on the estimation is shown in Fig 10. Increasing the sampling interval to 0.2 s results in an accurate estimation of the quasi-steady derivatives. Obviously the model structure given by equation (4) is inadequate for portraying the short term

dynamic effects of the flapping equation (1), which in this case produces a mode with frequency 5.5 rad/s and time to half amplitude of about 0.1 s. A comparison of pitch rate response using the full equations and the quasi-steady representation is illustrated in Fig 11. Clearly the angular acceleration in the former case is zero at the origin and builds up to the quasi-steady value after about 0.2 s. Using data in this interval for estimating quasi-steady derivatives tends, therefore, to underestimate the damping in the motion to the extent that for, very short data lengths, an unstable system is predicted as shown in Fig 9.

When analysing flight data one would, of course, use a much longer data record than used in the previous example and the step input is rather limited in its excitation spectrum. However, a multi-step input would typically extend over about 30% of the data record and the contamination effects described above might persist well into the record.

Several other attempts to identify 6 dof helicopter models have resulted in underestimation of primary damping derivatives relative to the quasi-steady values (Refs 11-13). All these references report using advanced statistical methods for estimating derivatives but the phenomenon is still present in the results. The obvious solution to the problems highlighted by Molusis is to measure individual blade motions and to use higher order model structures in the estimation process. There will obviously be flight cases when such a solution is mandatory to the identification of certain phenomena, particularly when 6 dof theoretical models are known or suspected to be inadequate. For a wide range of conditions within the normal flight envelope, however, it is hoped that 6 dof models can be used to predict handling characteristics adequately and it is worthwhile exploring other potential solutions to the data processing problems before resorting to the measurement of blade motions. One approach is to use an input signal with a frequency content that excludes the rotor modes. A possible shortcoming of this method is that the data could be starved of information necessary to predict some of the derivatives, particularly for hingeless rotor helicopters where the lower frequency rotor modes are not far removed from some of the body modes. Nevertheless, the use of smooth inputs rather than sharp steps or ramps has an obvious appeal in this context. A similar and perhaps complementary solution involves filtering the data to exclude the 'higher' frequency content but again this could mean coming down to frequencies as low as $\frac{1}{2}$ Hz. Some exploratory work was done on this theme by one of the present authors in Ref 14, where the estimation process was transferred to the frequency domain. The data can then be filtered by excluding data beyond the frequency range of interest. This idea will now be exploited for the analysis of the Puma data.

Current Methods

The techniques used in this paper are based on the system identification approach described in Ref 15, where the data analysis is divided into three main stages; state estimation, model structure estimation and parameter identification. The state estimation stage involves the reconstruction of all states and controls from the available sensor measurements using a Kalman filter/smoother[16]. This process also eliminates the biases and scale factor errors from the measured data and reduces the level of measurement noise. The second stage utilises a stepwise least squares regression technique[17] to derive an adequate model structure from a range of possible candidates. The method uses certain statistical criteria to determine which states should be included in the model and estimates the corresponding coefficients. The third stage adopts these estimates as starting values for a maximum likelihood estimation process that generates unbiased, efficient, parameter estimates.

The analysis of results described in the next section will be confined to the first two stages described above. The equations used in the state estimation process are essentially kinematic relationships. For the present data set the reconstructed states include the three velocity components and the translational and rotational accelerations of the aircraft centre of gravity. The external forces and moments are then directly related to the acceleration estimates and for the model structure estimation we choose the 6 dof formulation of the form

$$\underset{\sim}{F} = A\underset{\sim}{x} + B\underset{\sim}{u} \qquad (7)$$

$\underset{\sim}{F}$, $\underset{\sim}{x}$ and $\underset{\sim}{u}$ are the external force and moment vectors, vehicle state vector and control vector respectively. The regression process currently used treats each equation separately, but rather than find the coefficients of this limited model that are valid for the entire frequency range of the data, it is more appropriate to determine the best set for the frequency range of interest. This is readily accomplished by transforming the data to the frequency domain using a Fast Fourier Transformation (FFT) and then truncating the data beyond the bandwidth of interest. If it is

assumed that the coefficients do not vary with frequency then the regression can be performed in the frequency domain with the vectors in equation (7) interpreted as the corresponding Fourier transforms. An additional advantage of estimation in the frequency domain is that the resolution can be improved by padding the data with zeros. This effectively forces the spectral lines to be more closely spaced without affecting the frequency content of the data. The higher resolution should result in more accurate estimation of the low frequency modes, which are difficult to identify from a limited duration data record[14].

Model Structure Estimation with Puma Data

The results presented in this section were produced at the Ames Research Center and forwarded to RAE Bedford for interpretation. The inherent communication difficulties in this process limited the scope of this first phase of the collaboration. The analysis software is currently being implemented on a VAX computer at Bedford when these difficulties should be largely overcome.

From the assortment of data collected during Puma flight 325, three manoeuvres were selected for analysis, namely doublet inputs in lateral cyclic, pedal and longitudinal cyclic. The data used consisted of measurements from one of the packs of inertial instruments (accelerometers, rate gyros, attitude gyros), the airspeed sensor and the pitch and yaw vanes. The instrument pack referred to included a 2-pole Butterworth filter ($\omega_n \sim 10.6$ Hz , $\zeta = 0.73$) that effectively removed the dominant 4/rev noise in the measurements. The results of the model structure estimation process reveal a marked variation in estimated coefficients, particularly the contributions from coupling effects. The reasons for this are not yet understood and we therefore choose to concentrate on a synthesis of the primary moments for each input, *ie* rolling moment for lateral cyclic doublet, yawing moment for pedal doublet and pitching moment for the longitudinal cyclic doublet. The sample rate for all channels was 64/s, a rate that limited the record lengths to about 15 s. This limitation will be removed in future analysis. The results from each manoeuvre will be discussed in turn.

Lateral Cyclic Doublet/Rolling Moment Synthesis

Results from the filter/smoother process are shown in Fig 12, where it can be seen that only two cycles of the lateral oscillation are available. Two further points are worth noting; a bias has been detected and corrected for in the pitch rate gyro and the initial slope of the normal velocity component (w) indicates an initial climbing and decelerating flight condition. The effect of this unsteady initial condition has not been explored. In discussing the results of the model structure estimation we will refer to the multiple correlation coefficient (R) for the fit. In essence, the closer R^2 is to unity, the better the overall fit of the data in the frequency domain. Table 5 summarises the estimated rolling moment coefficients (derivatives) for the cases studied, along with the current quasi-steady theoretical predictions. Derivative estimates with a structure containing only lateral variables are compared for three frequency ranges, 0 to 0.5 Hz, 0 to 1 Hz, 0 to 4 Hz. In all cases the high R^2 values indicate a reasonably good fit with this limited model. The roll damping L_p is seen to increase by about 50% as the bandwidth is reduced but is still markedly lower than the theoretical prediction. The Fourier transform of the rolling moment is compared with the estimated fit in Fig 13, for the two lower frequency ranges. Most of the data is contained in the range 0 to 0.5 Hz, and the dominant peak at 0.25 Hz corresponds to the lightly damped lateral oscillation. The fairly close fit at and above this frequency appears to be achieved at the expense of the fit at lower frequencies. Referring again to Table 5, it can be seen that R^2 rises to 0.96 when the longitudinal variables w and q are added, with some associated modification to the lateral variable coefficients. Comparing the estimated and theoretically predicted derivatives in Table 5 we can see that the major anomalies are for the rate derivatives L_p and L_r . The magnitude of these effects seems to have been reversed for the flight results but it is difficult to rationalise the physical significance of this; indeed the result seems rather dubious. Further exploration into the details of the regression analysis is clearly required.

Pedal Doublet/Yawing Moment Synthesis

The smoothed state estimates for this manoeuvre are illustrated in Fig 14 and the yawing moment derivatives derived from the lower frequency bandwidth of data are compared with theoretical predictions in Table 6. Results from two different model structures are included, one with lateral variables only and the other with the addition of the longitudinal variables w and q . The multiple correlation coefficient is hardly affected by these additions.

It can be seen that the directional stiffness (N_v) and damping (N_r) compare very well with theory but the control power (N_{η_p}) is somewhat larger according to theory. The most striking differences are in the coupled rate derivatives N_p and N_q. The small value of N_p predicted by theory is the result of the cancellation of two larger effects from the main (negative N_p) and tail-rotor (positive N_p). It is interesting to note that the value of R^2 was raised to 0.91 by the first two variables drawn into the regression, v and η_p, the remaining variables then being added to account essentially for the out of phase component of the response. For the lightly damped yawing mode the sum of these contributions should obviously be small. Once again, a detailed breakdown of the in-phase and quadrature components of these 'damping' terms is required to aid further interpretation of the results.

Longitudinal Cyclic Doublet/Pitching Moment Synthesis

The state estimates derived for this manoeuvre are shown in Fig 15, where the bias error in the pitch rate gyro is again apparent; also the normal and longitudinal velocity estimates again indicate an initial decelerating climb. The least squares estimates in the frequency domain are compared, in Table 7, with the quasi-steady theoretical predictions for the derivatives. Results are presented for the longitudinal model structure for the three frequency ranges. Both the pitch damping (M_q) and control power ($M_{\eta_{1s}}$) are seen to increase as the bandwidth is reduced and both rise to nearly 80% of the theoretical predictions. The remarkable agreement for the speed stability derivative (M_u) is somewhat overshadowed by the incidence stability derivative (M_w) comparison. The variable w actually just managed to become part of the fit, accounting for only the last few per cent in the value of R^2. It is possible that the estimation of an unstable M_w is related to the unsteady initial conditions for this manoeuvre, as the effects of the initial deceleration persist for the duration of the record as shown in Fig 15. It is intended to explore this topic further.

The results from the three manoeuvres discussed above are both encouraging and perplexing. Unfortunately, time was not available to explore further the uncovered anomalies, for this paper. The underestimation of roll damping, relative to theory, a feature common to several earlier attempts at rotorcraft parameter estimation, is perhaps of greatest concern. The reduction effect of the lower frequency flapping modes, described in an earlier section, should be minimized by truncation in the frequency domain. The least squares regression analysis does of course have its shortcomings, particularly when noise is present in the data[18], but also when there is strong correlation between states. However the technique is appealing in that it offers a simple and systematic approach to model structure estimation, and investigations of the type described above will be pursued in the continuing collaborative programme. When fully exploited and understood, the results of the model structure estimation stage will then be used to initiate the more complex maximum likelihood process.

The model structure estimation stage serves another useful purpose in the validation of reduced order approximate models of helicopter flight mechanics. Simplified models, which still indicate trends accurately, have obvious advantages and various schemes are suggested in the Appendix for the 6 degree of freedom helicopter as a framework for analytic model reduction. The results described are based on the theoretical predictions of Puma characteristics discussed earlier in the paper. Clearly, however, we have failed to validate the theoretical arguments put forward to explain the low damping of the lateral oscillation. In particular, the yawing moment derivatives N_w and N_q in Table 6 bear little resemblance to their theoretical counterparts, and, unfortunately for this study no estimate was obtained for the derivative M_p (another important effect in the theory). There is no reason to believe that any major physical effect has been neglected in the theoretical quasi-steady derivatives, but it is possible that the omission of the rotorspeed degree of freedom has distorted the model structure estimation. With this possibility in mind, future estimations will include this additional state.

Concluding Remarks

Results from the first phase of an RAE/NASA collaborative programme in rotorcraft system identification have been described. Flight data from three manoeuvres with an RAE Puma helicopter have been processed by the state estimation and model structure estimation processes of a NASA system identification software package. A comparison of moment derivative estimates with theoretical predictions has been used as a guide to the likely accuracy involved. No firm conclusions can be drawn from this first exploration but a number of features are worth highlighting.

(1) Encouraging results have been obtained by performing the regression analysis in the frequency domain. Reducing the bandwidth of data used resulted in an increase in roll and pitch damping and control power, as expected from time domain considerations,

but, in some cases, the results still fall well short of expected quasi-steady values.

(2) Primary yawing moment derivatives estimated from a pedal doublet manoeuvre show good agreement with theory but the adverse yaw (N_p) and coupling from longitudinal motion (N_w,N_q) show significant differences. The contribution of these coupling terms to the 'dutch roll' mode damping, so elegantly expressed by simple theory, cannot, therefore, be substantiated.

(3) Roll damping (L_p) and control power ($L_{\eta_{1c}}$) estimated from a lateral cyclic doublet manoeuvre are considerably lower than theory predicts - a result in keeping with previous reports. This anomaly in the rolling moment is accompanied by a very high estimate for the derivative L_r and the temptation at this stage is to question the structure estimation, rather than theory, for these effects.

(4) The closest agreement with quasi-steady predictions were obtained for pitching moment derivatives from a longitudinal cyclic doublet manoeuvre, except for the static stability derivative M_w which is estimated to be very small and positive by the least squares regression.

(5) A theoretical framework for exploring reduced order model structures has been outlined in an Appendix to the paper. A coupled longitudinal/lateral fourth order system is required to describe the current theoretical predictions of the Puma 'dutch roll' oscillation.

The collaborative programme is still at an early stage and more detailed investigations using the model structure estimation process are planned for different manoeuvres of longer duration and possibly improved model structures.

Appendix

The Use of Reduced Order Theoretical Models

The complex nature of helicopter flight mechanics make it a prime candidate for treatment as a sum of interacting subsystems, with the attraction that phenomena may be described by considering a series of lower order problems and their interactions. Conditions under which this type of approximation is valid are often based on intuitive reasoning but they can be formulated more precisely using notions of subsystem dynamic separation (eg widely separated characteristic times) and interaction strength. For aircraft flight dynamics such opportunities often arise for describing rigid body/aeroelastic interaction or in the description of the individual modes using familiar arrangements of motion variables, eg longitudinal short period mode made up of incidence and pitch rate excursions. Once again, the attractions of performing such a 'partitioning' analysis can often stem from the enhanced physical appreciation it inspires. In this Appendix we concentrate on the theoretical results discussed earlier and outline a framework for reduced order analysis. One can clearly imagine the 6 dof model as already being a reduced order approximation of a higher order system containing rotor as well as engine/fuel control system degrees of freedom.

The method of analysis is described in Ref 19 where the concept of weak coupling is introduced and conditions of application are quantified. The technique has been applied to strongly controlled aircraft motions[20] and more recently to describe the range of application of the longitudinal short period approximation for helicopters[21]. In the present paper, a form of approximation for lateral/directional motion is sought. For the Puma results described the strong coupling from longitudinal motion renders the search in vain. In the following, aspects of open loop stability characteristics only will be addressed.

The reduction process is based on a partitioning of the system matrix into lower order subsystems that are weakly coupled. Details of the method can be found in any of the references cited above and will not be elaborated upon here. In order to achieve the correct partitioning for rigid body modes of motion we need to introduce the vertical velocity w_0 and sideways velocity v_0 as new variables, replacing pitch attitude and yaw rate in the equations of motion. The system matrices, in partitioned form, for decoupled longitudinal and lateral motions are shown in Table 8, along with the approximating characteristic polynomials. One would not expect these formulae to give very accurate results in general but they do serve as a yardstick against which the effects of coupling terms can be measured. For the Puma derivative data given in Table 3 the weakly coupled approximate results are shown in Table 9.

A comparison with the decoupled longitudinal/lateral results given in Table 4 indicates again that the dutch roll damping is badly overpredicted. This poor comparison will result when the oscillatory sideslip motion has a significant component of sideways motion superimposed on the sideslip due to yawing motion. The overprediction of the phugoid damping can be attributed to a similar effect in the longitudinal plane. For the other three modes the approximations are clearly satisfactory. The importance of the directional stiffness N_v on the dutch roll damping is not, of course, predicted at all by this type of approximation. The root loci in Fig 16 illustrates this effect; the two curves

shown are for the coupled longitudinal/lateral system and for the lateral system alone. Both loci are approaching the asymptotic value given in Table 9 as N_v increases, ie dutch roll damping $\simeq (N_r + Y_v)$. The point being made is that as directional stability increases the formulae given in Table 8 are not only becoming better approximations to the lateral subset damping but that both are improving relative to the fully coupled result. In these conditions the other modes are also approximated fairly accurately, eg spiral mode marginal stability is well predicted, although these results are not shown here.

The results discussed above indicate that the degree of coupling between longitudinal and lateral motion can be strongly influenced by the directional stiffness or, in other words, by the frequency of the lateral oscillation. This result is somewhat intuitive and for the present coupled system the coincidental similarity between the longitudinal short period and dutch roll frequencies is bound to result in strong longitudinal/lateral interactions. As discussed in an earlier section these interactions are brought about mainly through the derivatives M_p and N_w ; the main rotor contribution to these derivatives being negative and positive respectively for 'clockwise' rotating rotors. The strong coupling present leads to a further reduction in dutch roll damping through the mechanism discussed earlier. This effect can be quantified by considering a reduced order system made up of both the longitudinal and lateral 'fast' oscillatory modes.

Assuming on the one hand that translational velocity excursions (u, v_0, w_0) are much slower and weakly coupled, and, on the other, that the roll subsidence approximation interacts in a quasi-steady manner, the 4th order approximate system takes the form,

$$\frac{d}{dt}\begin{bmatrix} w \\ q \\ v \\ \dot{v} \end{bmatrix} - \begin{bmatrix} Z_w & Z_q + U_e & 0 & 0 \\ M_w & M_q & -M_p L_v/L_p & M_p L_r/U_e L_p \\ 0 & 0 & 0 & 1 \\ -N_w U_e & 0 & -\left(U_e N_v + (L_v/L_p)(g - N_p U_e)\right) & N_r + Y_v + (L_r/L_p)(g - N_p U_e) \end{bmatrix} \begin{bmatrix} w \\ q \\ v \\ \dot{v} \end{bmatrix} = Q. \qquad \ldots\ldots(8)$$

Here we have neglected all coupling terms except M_p and N_w , but with the strong coupling remaining, no further reduction would be reliable. Examination of the Routhian for this 4th order system indicates that the oscillatory stability boundary is crossed when $N_w \sim 0.02$, which is in accordance with the results presented earlier in Fig 6. The eigenvalues for the above system are,

$$\lambda_{\text{short period}} = -1.0 \pm 1.079i$$

$$\lambda_{\text{dutch roll}} = -0.114 \pm 1.115i$$

giving the right order of damping reduction for the dutch roll mode. If we assume a neutrally stable oscillation exists for the above system then a good approximation to this damping decrement can be obtained by deriving the steady state frequency response of equation (8). For this case w is approximately 180^0 out of phase with $\dot{v}$ (hence in phase with yaw rate) and the effective damping becomes,

$$\text{damping}_{(\text{dutch roll})} \simeq -\left(N_r + Y_v + \frac{L_r}{L_p}(g - N_p U_e) + \frac{N_w M_p}{L_p \omega_0}\frac{U_e^2 L_v}{(Z_w + M_q)}\right) \qquad \ldots\ldots(9)$$

$$\simeq 0.234 ,$$

hence

$$R_e(\lambda) \simeq -0.117$$

(where ω_0 is the dutch roll frequency)

which agrees with the result given by equation (8) above.

The derivative N_w , as stated earlier, represents the quasi-steady torque variation produced by the engine, in response to rotorspeed variations. The validity of this implicit weak coupling assumption can only be assessed when an engine/rotorspeed control system model structure, representative of Puma, is incorporated. The derivative N_w itself is produced mainly by the 'induced torque', written in coefficient form,

$$C_{Q_i} = -C_T(\mu_z - \lambda_0) . \qquad (10)$$

C_T is the rotor thrust coefficient and $(\mu_z - \lambda_0)$ is the upwash, normal to the disc. The variation in the semi-normalised yawing moment (yaw acceleration), from this source, with normal velocity w is shown in Fig 17. The variation is seen to be moderately non-linear particularly in the normal helicopter working state ($w < 0$). The derivative N_w is seen to increase as autorotation is

approached ($\mu_z - \lambda_0 \sim 0$) but the effect will, of course, disappear once the engine disengages. It is known that the directional stiffness can also reduce in this region due to fin shielding effects; the loss of 'dutch roll' damping for these flight conditions should, therefore, be fairly severe if the current predictions are correct.

Acknowledgements

Grateful thanks are extended to colleagues by both authors for the help given in the preparation of material for this paper; in particular to Mustafa Demiroz and Susan Chu at NASA Ames and to Tony James and Jane Whitbread at RAE Bedford.

References

1. Padfield, G.D. "A Theoretical Model of Helicopter Flight Mechanics for Application to Piloted Simulation." RAE Technical Report 81048, Apr. 1981.

2. Padfield, G.D., Tomlinson, B.N., Wells, P.M. "Simulation Studies of Helicopter Agility and other topics." RAE Technical Memorandum

3. Sarconi, G. "Simulation Hélicoptere caracteristique du SA 330." Aerospatiale Note Technique, 330.05.0080, 1975.

4. Hoerner, S.F., Borst, H.V. Fluid Dynamic Lift, Hoerner Fluid Dynamics, N.J., 1975.

5. Roesh, P., Vuillet, A. "New Designs for Improved Aerodynamic Stability in Recent Aerospatiale Helicopters." Proceedings of the 37th AHS Annual Forum, New Orleans, May 1981.

6. Kuczynski, W.A., et al. "The Influence of Engine/Fuel Control Design on Helicopter Dynamics and Handling Qualities." Proceedings of the 35th AHS Annual Forum, Washington, May 1979.

7. Parameter Identification, AGARD Lecture Series 104, Nov. 1979.

8. Molusis, J.A. "Helicopter Stability Derivative Extraction and Data Processing Using Kalman Filtering Techniques." 28th AHS National Forum, Washington, May 1972.

9. Molusis, J.A. "Helicopter Stability Derivative Extraction from Flight Data Using the Bayesian Approach to Estimation." Journal of the American Helicopter Society, Jul. 1973

10 Molusis, J.A. "Rotorcraft Derivative Identification from Analytical Models and Flight Test Data." AGARD CP 172 (Methods for Aircraft State and Parameter Identification)." Nov. 1974.

11 Kaletka, J., Rix, O. "Aspects of System Identification of Helicopters." Proceedings of the 3rd European Rotorcraft and Powered Lift Aircraft Forum, Aix-En-Provence, France, Sept. 1977.

12 Kloster, M., Kaletka, J., Schaufele, H. "Parameter Identification of a Hingeless Rotor Helicopter in Flight Conditions With Increased Instability." Proceedings of the 6th European Rotorcraft and Powered Lift Aircraft Forum, Bristol, UK, Sept. 1980.

13 Hodge, Ward, "Comparison of Analytical and Flight Test Identified Aerodynamic Derivatives for a Tandam Rotor Transport Helicopter." NASA TP-1581, Feb. 1980.

14 DuVal, R.W. "The Use of Frequency Methods in Rotorcraft System Identification." First AIAA Flight Testing Conference, Paper 81-2386, Las Vegas, Nov. 1981.

15 Hall, W. Earl, Jr., Gupta, Narendra K., Hansen, Raymond S., "Rotorcraft System Identification Techniques for Handling Qualities and Stability and Control Evaluation." Proceedings of the 34th AHS National Forum, Washington, May 1978.

16 Bryson, A.E., Jr., Ho, Y.C. "Applied Optimal Control, Blaisdell Publishing Co. Waltham, Mass, 1969.

17 Jennrith, R.I. "Stepwise Regression." Statistical Methods for Digital Computers, Wiley, NY, 1966.

18 Fiske, Philip H., Price, Charles F. "A new Approach to Model Structure Identification." AIAA Paper 77-1171, 1977.

19 Milne, R.D. "The Analysis of Weakly Coupled Dynamical Systems." Int. J. Control, 2, No.2, 1965.

20 Milne, R.D., Padfield, G.D. "The Strongly Controlled Aircraft." Aeronautical Quarterly, May 1971.

21 Padfield, G.D. "On the Use of Approximate Models in Helicopter Flight Mechanics." Vertica, Vol 5, pp. 243-259, 1981.

Nominal* IAS	100 kn
Relative density, σ	0.818-0.837
Rotorspeed, Ω	26.6-27.2 rad/s
Rotor torque ~	11500 ft lb (564 hp, 421 kW)
AUW	13018-12169 lb (5904-5519 kg)
I^{**}_{xx}	6380 slug ft^2 (8650 kg m^2)
I^{**}_{yy}	25483 slug ft^2 (34550 kg m^2)
I^{**}_{zz}	20283 slug ft^2 (27500 kg m^2)
Cg location below rotor hub	7.05 ft (2.157 m)
Cg location forward of rotor hub	0.086 ft (0.026 m)
Rotor Lock number	7.86
λ^2_β	1.0516
Solidity, s	0.0917

* Actual IAS varied from 95-100 kn giving an EAS ~ 105-110 kn.
** Manufacturer's estimates (Ref 3).

Table 1. Puma flight 325 — nominal trim conditions

Parameter	Flight (approx)	Theory
Period (s)	4.5	6.0
$T_{\frac{1}{2}}$ (s)	14.0	15.36
$\lvert p/v \rvert$	0.02	0.019
$\angle p/v$	135°	158°
$\lvert r/v \rvert$	0.012	0.0096
$\angle r/v$	-95°	-85°
$\lvert q/v \rvert$	0.006	0.0027
$\angle q/v$	98°	-48°
$\lvert w/v \rvert$	0.336	0.354
$\angle w/v$	30°	-107°

Table 2. Comparison of measured and predicted 'dutch roll' oscillation characteristics

	u	w	q	v	p	r
X	-0.2650E-01	-0.9340E-03	0.3970E 01	0.1890E-02	0.1010E 01	0.0000E 00
Z	-0.3190E-01	-0.7050E 00	0.1680E 03	0.1450E-01	0.2100E 01	0.0000E 00
M	0.2460E-02	-0.5570E-02	-0.8310E 00	-0.4000E-03	-0.2070E 00	0.0000E 00
Y	-0.8120E-02	0.2930E-02	0.1040E 01	-0.1360E 00	-0.3980E 01	-0.1680E 03
L	-0.5620E-02	-0.2730E-03	0.8390E-00	-0.2200E-01	-0.2050E 01	0.2940E 00
N	0.2880E-02	0.1270E-01	-0.3280E 00	0.6050E-02	-0.9290E-03	-0.5280E 00

Table 3. Theoretical estimates of Puma derivatives

Mode	Coupled system	Decoupled long/lat subsystems
Roll subsidence	-2.242	-2.209
'Dutch roll'	-0.0451 ±1.047i	-0.193 ±1.079i
Spiral	-0.1166	-0.1194
'Short period'	-0.9054 ±1.186i	-0.7645 ±0.9354i
'Phugoid'	-0.00833 ±0.1764i	-0.0168 ±0.2038i

Table 4. Comparison of coupled and uncoupled longitudinal/lateral system eigenvalues — Puma, 100 kn

	Flight estimates lateral variables only			+ w and q	Theory
	0-0.5 Hz	0-1 Hz	0-4 Hz	0-0.5 Hz	
R^2	0.92	0.91	0.9	0.96	
L_v	-0.013	-0.013	-0.013	-0.0123	-0.022
L_p	-0.4	-0.32	-0.28	-0.35	-2.05
L_r	1.7	1.82	1.9	3.03	0.294
$L_{\eta_{1c}}$	0.022	0.021	0.02	0.019	0.044
L_w				0.0054	-0.00027
L_q				1.39	0.839

Table 5. Rolling moment derivatives — estimates from flight and theory

	Flight estimates (0-0.5 Hz)		Theory
	Lateral variables only	+ w and q	
R^2	0.97	0.98	
N_v	0.0053	0.0071	0.00605
N_p	-0.6	-0.53	-0.0009
N_r	-0.636	-0.572	-0.528
N_{η_p}	-0.027	-0.028	-0.043
N_w		-0.003	0.0127
N_q		0.322	-0.328

Table 6. Yawing moment derivatives — estimates from flight and theory

	Flight estimates			Theory
	0–0.5 Hz	0–1 Hz	0–4 Hz	
R^2	0.802	0.76	0.73	
M_u	0.00243	0.00243	0.00245	0.00246
M_w	0.00092	0.00085	0.00074	−0.0056
M_q	−0.683	−0.667	−0.648	−0.831
$M_{\eta_{1s}}$	0.0316	0.0302	0.029	0.038

Table 7. Pitching moment derivatives — estimates from flight and theory

(Note $\overleftrightarrow{M_w(Z_q + U_e)} = M_w(Z_q + U_e) - M_q Z_w$)

Longitudinal subset $\underset{\sim}{X} = \{u, w_o, w, q\}$; $w_o = w - U_e\theta$

$$\left[\begin{array}{cc|cc} X_u & g/U_e & X_w - g/U_e & X_q - W_e \\ Z_u & 0 & Z_w & Z_q \\ \hline Z_{\dot{u}} & 0 & Z_w & Z_q + U_e \\ M_u & 0 & M_w & M_q \end{array}\right]$$

$\lambda_{1,2}$ (phugoid);

$$\lambda^2 + \left\{ -X_u + \frac{\left(X_w - \frac{g}{U_e}\right)\left(\overleftrightarrow{M_u(Z_q + U_e)} + (X_q - W_e)\overleftrightarrow{Z_u M_w}\right)}{\overleftrightarrow{M_w(Z_q + U_e)}} \right\}\lambda - \frac{g}{U_e}\left(Z_u - \frac{\overleftrightarrow{Z_w M_u(Z_q + U_e)}}{\overleftrightarrow{M_w(Z_q + U_e)}}\right) = 0$$

$\lambda_{3,4}$ (short period); $\lambda^2 - (Z_w + M_q)\lambda - \overleftrightarrow{M_w(Z_q + U_e)} = 0$.

Lateral subset $\underset{\sim}{X} = \{\dot{v}_o, v, \dot{v}, p\}$; $\dot{v}_o = \dot{v} + U_e r$

$$\left[\begin{array}{c|cc|c} 0 & 0 & Y_v & g \\ \hline 0 & 0 & 1 & 0 \\ -N_{\dot{r}} & -U_e N_v & N_r + Y_v & g - N_p U_e \\ \hline L_{\dot{r}}/U_e & L_v & -L_{\dot{r}}/U_e & L_p \end{array}\right] \quad (Y_p = Y_{\dot{r}} = 0)$$

λ_5 (spiral) ; $\lambda = \dfrac{g}{U_e}\dfrac{\overleftrightarrow{L_v N_{\dot{r}}}}{\left(\overleftrightarrow{L_p N_v} + \frac{g}{U_e} L_v\right)}$

$\lambda_{6,7}$ (dutch roll); $\lambda^2 - \left(Y_v + N_r + \frac{L_{\dot{r}}}{L_p}\left(\frac{g}{U_e} - N_p\right)\right)\lambda + \left(N_v + \frac{L_v}{L_p}\left(\frac{g}{U_e} - N_p\right)\right)U_e = 0$

λ_8 (roll subsidence) ; $\lambda = L_p$

Table 8. Approximate formulae for longitudinal and lateral eigenvalues

Roll subsidence	−2.05
'Dutch roll'	−0.346 ±1.116i
Spiral	−0.1124
'Short period'	−0.768 ±0.968i
'Phugoid'	−0.0349 ±0.1969i

Table 9. Approximate eigenvalues for longitudinal and lateral subsystems

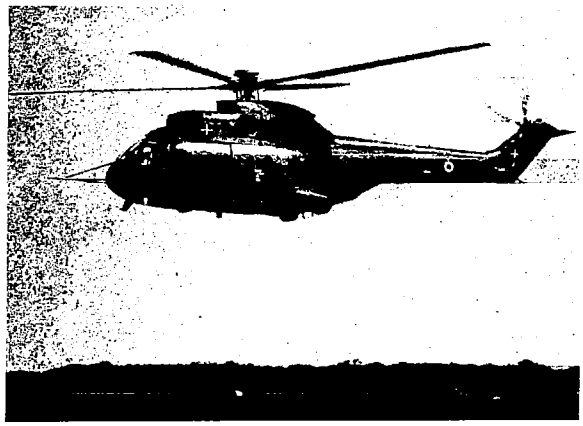

Fig 1 Puma XW241

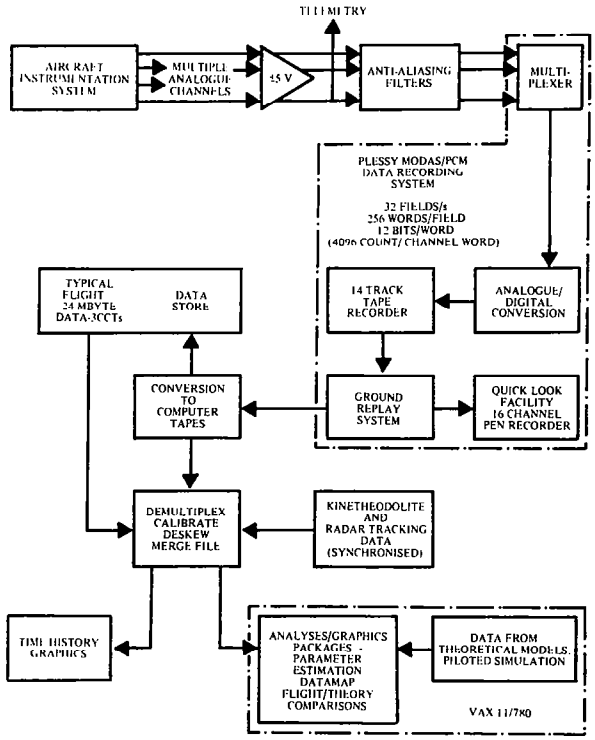

Fig 2 Puma flight mechanics data acquisition and processing at RAE Bedford

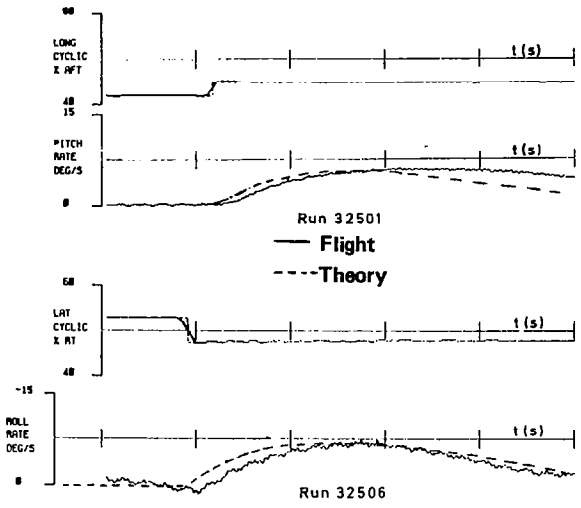

Fig 3 Flight/theory comparison of rate response to cyclic inputs

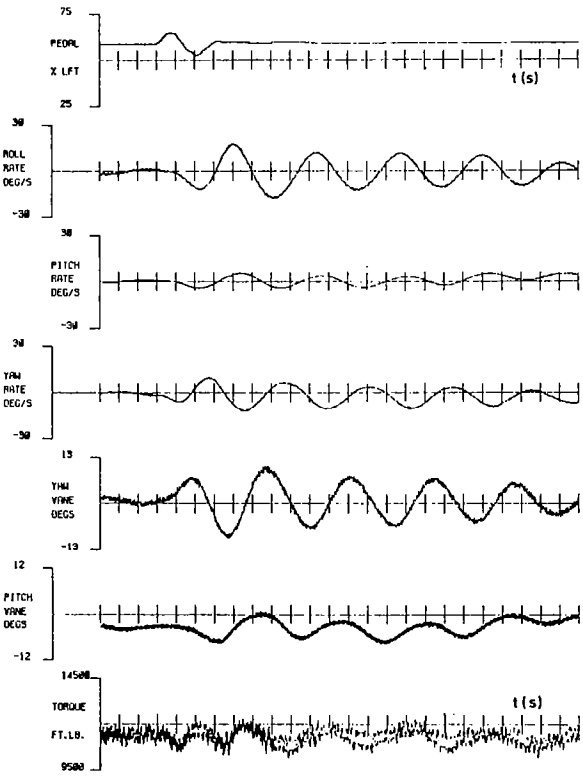

Fig 4 Puma flight 325, Run 12 — response to pedal doublet

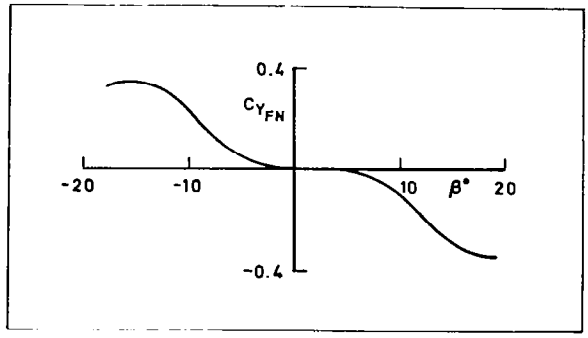

Fig 5 Puma fin sideforce coefficient vs sideslip angle

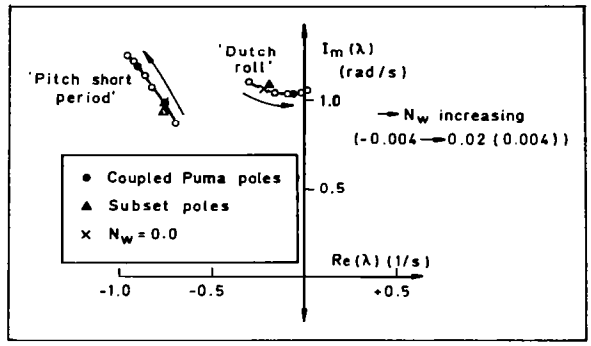

Fig 6 Root loci for fast oscillatory modes with varying yawing moment due to incidence (N_w)

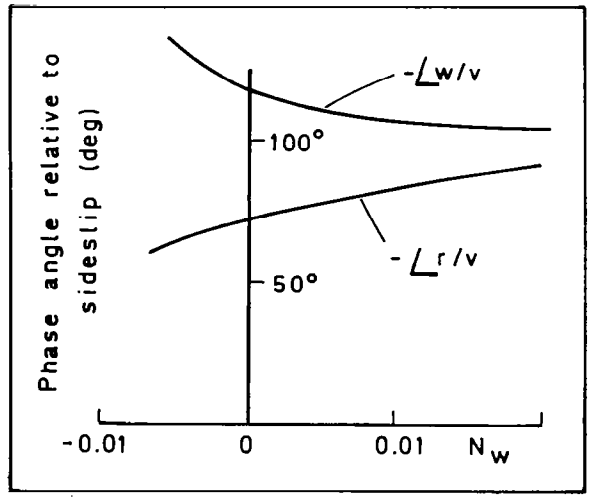

Fig 7 Variation of the phase angle in incidence and yaw rate excursions during 'dutch roll' oscillation with N_w — theoretical predictions

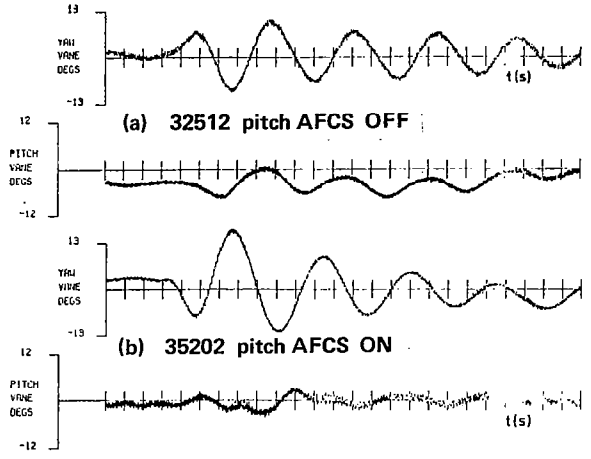

Fig 8 Puma — yaw and pitch vane response to pedal doublet

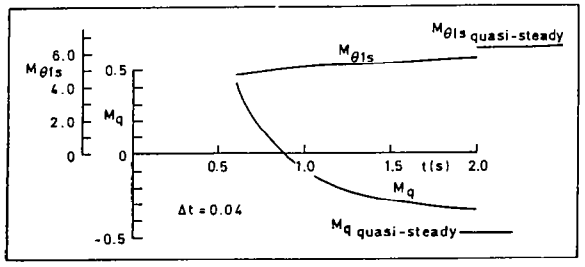

Fig 9 Variation of derivative estimates with record length

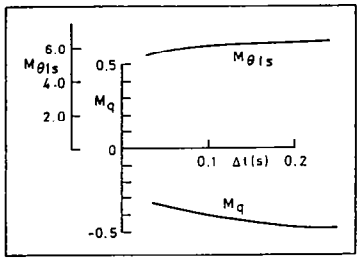

Fig 10 Variation of derivative estimates with sampling interval

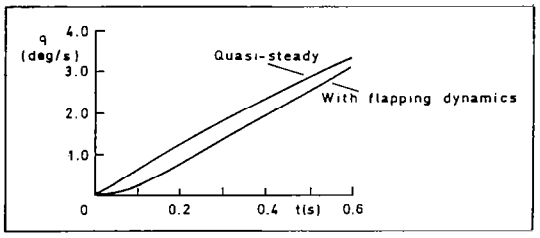

Fig 11 Comparison of pitch rate response with and without flapping dynamics

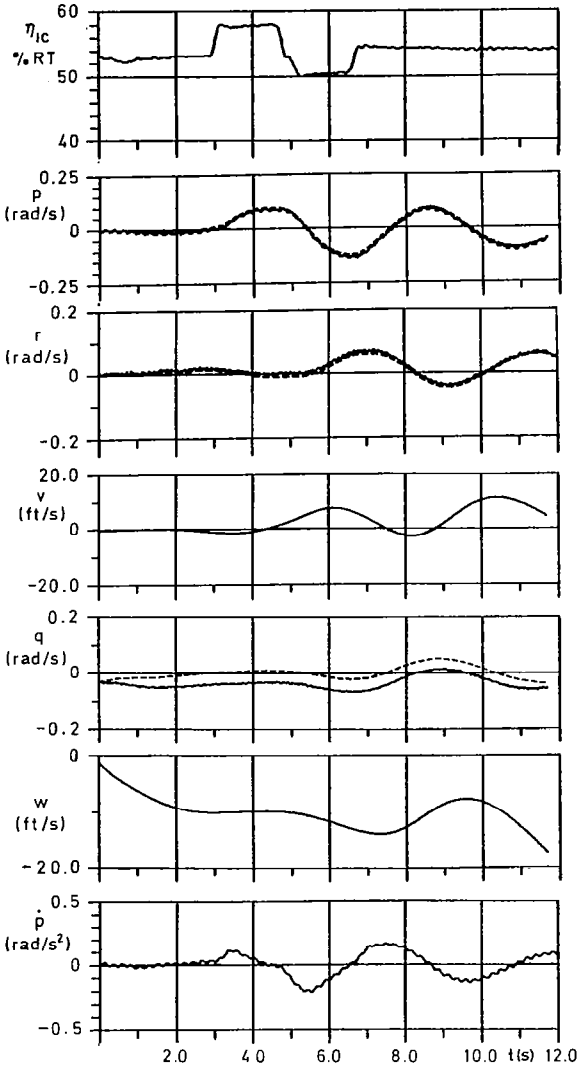

Fig 12 Comparison of measured (—) and estimated (- - -) states (Kalman filter/smoother) for lateral cyclic doublet manoeuvre

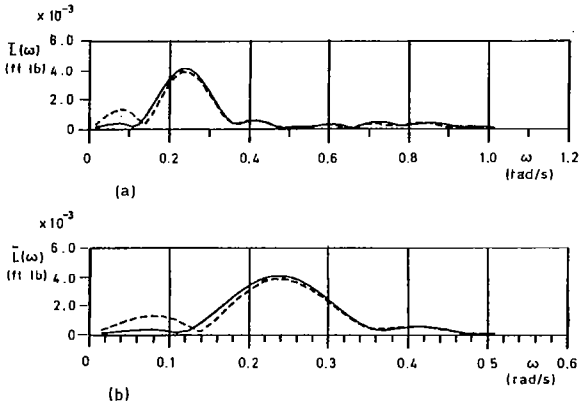

Fig 13 Fourier transform of measured (—) and estimated (- - -) rolling moment — lateral cyclic input

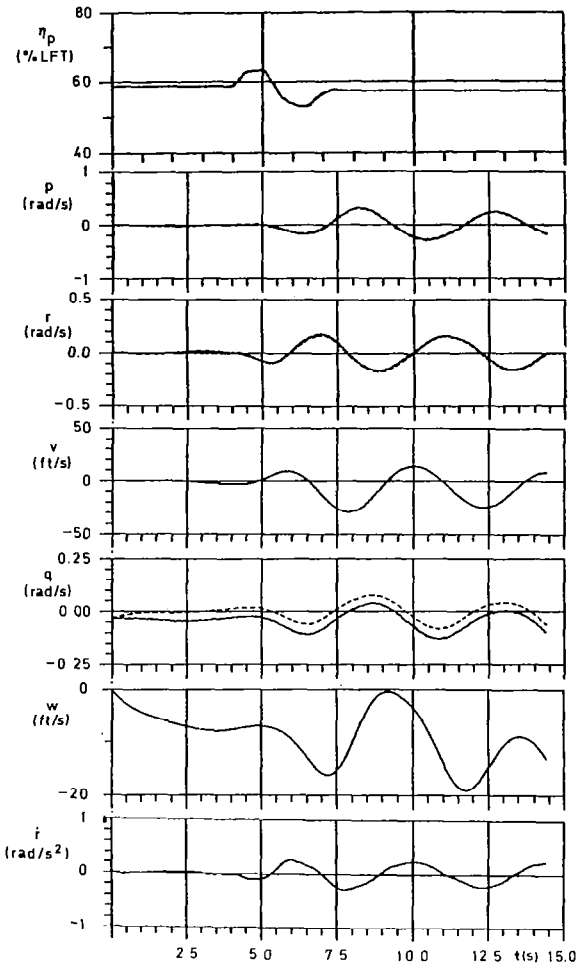

Fig 14 Comparison of measured (—) and estimated (- - -) states (Kalman filter/smoother) for pedal doublet manoeuvre

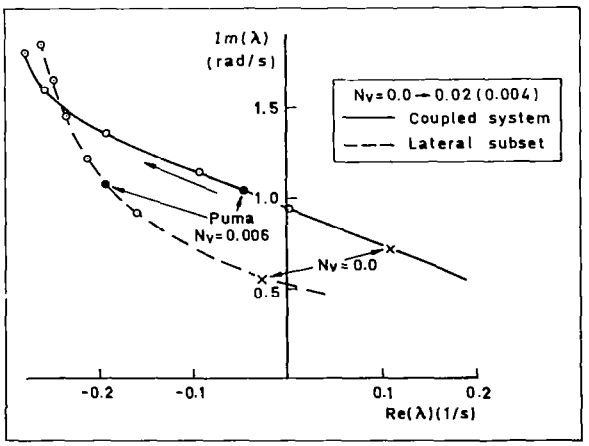

Fig 16 Root loci for 'dutch roll' mode with varying N_v — comparison of coupled and lateral/directional subset modes

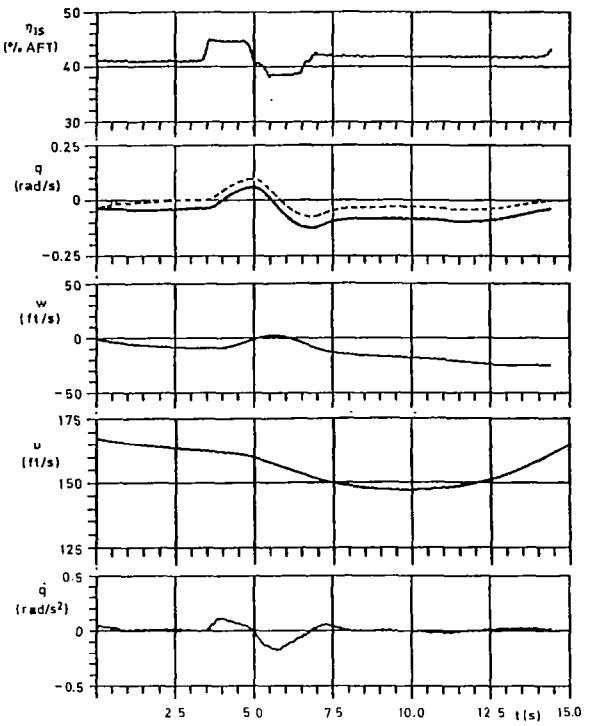

Fig 15 Comparison of measured (—) and estimated (- - -) states (Kalman filter/smoother) for longitudinal cyclic doublet manoeuvre

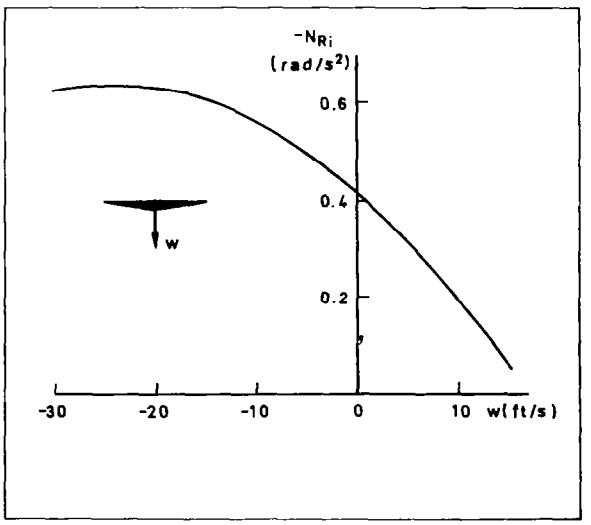

Fig 17 Variation of 'induced' rotor torque reaction with normal velocity perturbations